Composites: Part A 169 (2023) 107537

Contents lists available at ScienceDirect

Composites Part A

journal homepage: www.elsevier.com/locate/compositesa

Poly(ethylene-co-methacrylic acid) coated carbon fiber for self-healing composites

Mónica Peñas-Caballero [a], Enrico Chemello [b], Antonio Mattia Grande [b], Marianella Hernández Santana [a], Raquel Verdejo [a], Miguel A. Lopez-Manchado [a,*]

[a] Instituto de Ciencia y Tecnología de Polimeros (ICTP), CSIC, c/ Juan de la Cierva, 3, 28006-Madrid (Spain)
[b] Department of Aerospace Science and Technology, Politecnico di Milano, Milan, Italy

ARTICLE INFO

Keywords:
Self-healing
Thermoset
Thermoplastic
Coating
FRPs

ABSTRACT

We describe a simple and scalable method for incorporating thermoplastic agents into fiber reinforced polymers (FRPs). Poly(ethylene-co-methacrylic acid) (EMAA) nanoparticles were successfully deposited on the surface of carbon fibers via spray coating. EMAA was finely distributed and exhibited strong adhesion to the fibers. The EMAA-coated carbon fibers improved the fracture toughness and provided the FRPs with self-healing ability. The resulting healing efficiency, based on the recovery of the interlaminar fracture toughness, was above 40 % and gradually decreased after three repair cycles. The repair mechanism of the system involves the inherent flow capacity of the thermoplastic and formation of interfacial bridging between the two damaged interphases. This methodology allows pure resin to be used without any chemical modification or adverse effects on its viscosity, and the coated fiber can be stored until use.

1. Introduction

Over the last decade, the addition of thermoplastic additives has proven to be an effective technique for producing self-healing fiber reinforced polymers [1–4]. Thermoplastic polymers can induce self-healing by molecular interfusion since the molecules of this polymer become mobile at temperatures above their glass transition temperature, T_g [5]. This strategy has several advantages: it uses commercially available resins; the healing agent is indefinitely dormant, thus enabling multiple healing processes; and it is readily applicable.

According to the miscibility of the phases (thermoplastic and thermoset), mixtures can be divided into two types: miscible and immiscible. Some miscible blends include polycaprolactone (PCL) in epoxy resins cured with an amine-type hardener [6,7] or polybisphenol A-co-epichlorohydrin [8]. In the case of immiscible blends, one of the thermoplastics mostly used in composite materials is poly (ethylene-co-methacrylic acid) (EMAA), since it forms covalent bonds with the epoxy resin during the curing reaction and the thermal expansion of EMAA is 7 times greater than that of the resin. During the repair stage, a pressure delivery mechanism results from the condensation reaction that takes place between the epoxy resin and EMAA. This reaction produces bubbles that promote the EMAA to swell, flow into the cracks, and then bond with the epoxy matrix, resulting in the effective repair of the damaged surface [9–11].

Several methodologies have been described for incorporating EMAA into composites [1,2,10,12–34], such as discrete particles [2,29], meshes [16], porous membranes [32], non-woven fabrics [13], films [30], rectangular-shaped patches [14], and fibers [17]. In addition, EMAA filaments have been stitched into the fiber laminates prior to resin infusion or wet lay-up [15,20,22,27,28]. All these studies have demonstrated the performance of EMAA as a healing agent, with healing efficiencies of up to 411 % of the Mode I interlaminar fracture toughness or efficiencies up to 110 % of the Mode II peak load [32]. These recovery ratios are equal to or higher than those reported for microcapsule and microvascular repair methodologies [30,35]. Recent research has shown that EMAA intercalation between the fiber layers is the most effective strategy, as it can stiffen the interlayer of the composites while providing an excellent self-healing function [33,36,37]. However, many of these methodologies may be difficult to implement industrially; EMAA pellets must be mechanically ground into fine powder at cryogenic temperatures [12,29] or hot extruded to obtain filaments [36]. Moreover, in some cases, the EMAA distribution is not homogenous and self-healing only occurs near its location, such as when EMAA is stitched over the fibers [36].

* Corresponding author.
E-mail address: lmanchado@ictp.csic.es (M.A. Lopez-Manchado).

https://doi.org/10.1016/j.compositesa.2023.107537
Received 28 December 2022; Received in revised form 9 March 2023; Accepted 22 March 2023
Available online 25 March 2023
1359-835X/

This paper presents a novel and versatile methodology for the incorporation of thermoplastics, involving the spraying of an EMAA nanoparticle dispersion on the surface of the carbon fibers. EMAA pellets are dissolved and precipitated in tetrahydrofuran (THF), resulting in a nanoparticle solution that can be easily sprayed. The EMAA-coated composite not only shows healing capacity, but also improves Mode I interlaminar fracture toughness. This methodology could easily be implemented at industrial level, where the EMAA coating could be considered as a functional sizing due to its homogeneity and long-term stability.

2. Materials and methods

2.1. Materials

The epoxy resin used in this study was Resoltech 1050/1053 s, a bicomponent system composed of diglycidyl ether of bisphenol F (DGEBF 50–80 %), diglycidyl ether of bisphenol A (DGEBA, 10–40 %), and 1,6 hexanediol diglycidyl ether, and the hardener of polioxialcalinoamine/n-aminoetilpiperacine/dietiletriamine. The resin and hardener were thoroughly mixed at a specified ratio of 100:35 in parts by weight, yielding a low-viscosity system suitable for infusion processes. According to the supplier's specifications, the curing reaction was performed at 60 °C for 16 h. Unidirectional carbon fiber tape of 12 k, 340 g/m^2 density, and 45 μm thickness was supplied by INP96. Poly (ethylene-co-methacrylic acid) (EMAA), Nucrel^{TM} 925 Acid Copolymer from Dow, was used as the healing agent.

2.2. Sample preparation

Fig. 1 shows the steps used to coat the carbon fibers with EMAA nanoparticles:1) dissolution of the thermoplastic phase, 2) cooling, and 3) spraying and drying of the carbon fibers. In step 1, EMAA was dissolved in THF at a concentration of 0.012 g/ml and the solution was heated at 50–60 °C under constant stirring in an ultrasonic bath for 15–20 min. In step 2, the solution was cooled in an ice bath and turned milky white owing to the formation of nanoparticles [38]. In step 3, the solution was sprayed onto the carbon fiber surface on both sides at the required concentration of 10 wt% in relation to the resin content in the composite, i.e. approximately 3 wt% in relation to the composite, using an air spray gun (RS PRO) with a 0.22 L tank and a 0.3 mm nozzle. The solution was sonicated before use to prevent agglomeration. The air gun was cleaned after every two or three sprays to avoid clogging of the nozzle. The coated carbon fibers were then dried at 66 °C in an oven to remove the solvent until the weight remained unchanged.

Composites with plain carbon fibers or EMAA-coated carbon fibers were prepared using vacuum-assisted resin infusion (VARI). The carbon fibers were placed unidirectionally and the infusion was made in the fiber direction. 4-ply laminates with a thickness of 1.2–1.4 mm were prepared for flexural and interlaminar shear strength (ILSS) tests and 14-ply laminates with a thickness of 4.5–4.6 mm for static interlaminar fracture toughness tests. For the latter, a Teflon thin film of 13 μm thickness was placed along the mid-plane to initiate the delamination of the composite. For the 4-ply laminates, all sheets contained EMAA-coated fibers, whereas for the 14-ply laminates the coated fibers were only laid in the 6 central sheets. The laminates were cured at 60 °C for 16 h, and then post-cured at 150 °C for 2 h in a hydraulic press to compact the sheets. All samples for mechanical testing were cut using a Neurtek Brillant 220 precision cutting machine.

Table 1 shows that the incorporation of EMAA nanoparticles resulted in a slight decrease in the carbon fiber weight fraction, less than 6 %, and a small increase in the thickness of the composites. This is due to the volume occupied by the EMAA on the fiber, which increases the thickness of the laminate. Similar results have been reported in the literature when thermoplastic additives were incorporated into the composite

Table 1
Carbon fiber (CF) weight fraction and thickness of the different composites.

	Sample	CF weight fraction (%)	Thickness (mm)
4-ply laminates	Uncoated CF	72	1.34 ± 0.07
	EMAA-coated CF	66	1.58 ± 0.05
14-ply laminates	Uncoated CF	75	4.20 ± 0.2
	EMAA-coated CF	72	4.60 ± 0.1

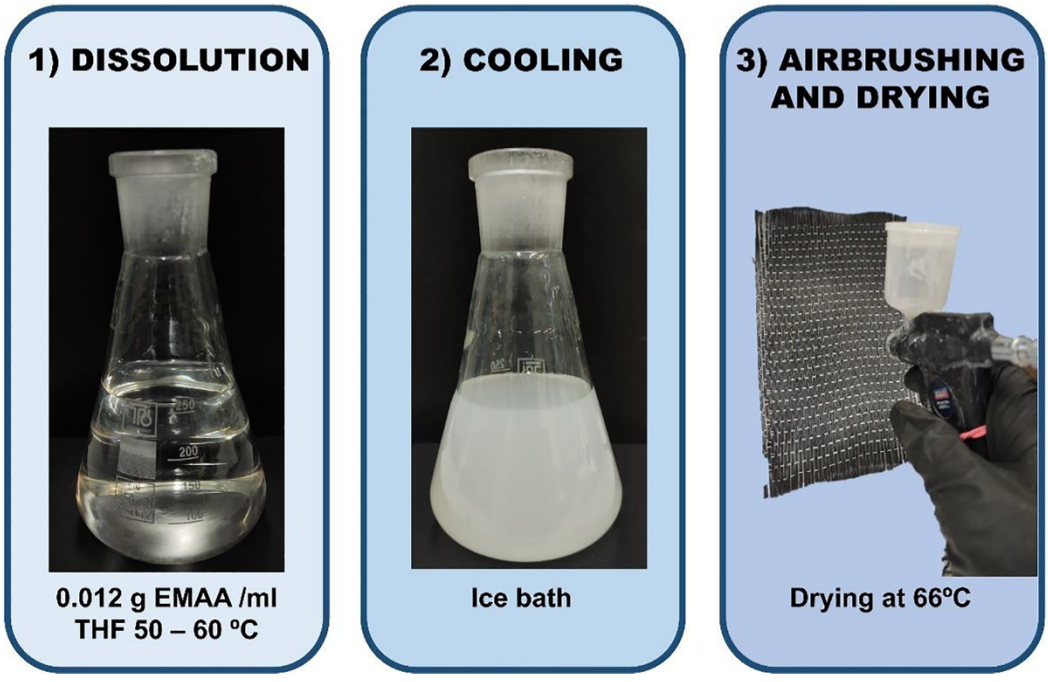

Fig. 1. Preparation of EMAA-coated carbon fibers: 1) Dissolution of EMAA in THF, 2) Cooling of the EMAA solution, and 3) Spraying of EMAA solution onto the carbon fiber surface.

[16,17,20]. However, the comparison of fracture toughness values between the composites is still valid, as it is not strongly dependent on the fiber content or thickness of the composite.

2.3. Characterization

The average particle size and surface charge of the EMAA nanoparticles were measured by dynamic light scattering (DLS) using a Malvern Nanosizer NanoZS instrument equipped with a 4 mW He-Ne laser ($\lambda = 633$ nm) and a scattering angle of 173°. The solution was analyzed in quartz cuvettes at 25 °C. Data were processed using Zeta-Sizer version 7.10 software, transforming the autocorrelation function into a size distribution based on the Stokes-Einstein equation.

The morphologies of the fibers were observed using an environmental scanning electron microscope (ESEM, Phillips, Model XL30) with a tungsten filament and an accelerating voltage of 25 kV. Prior to the observation, the samples were sputter-coated with gold/palladium (SC7640, Polaron).

The flexural properties and interlaminar shear strength (ILSS) of the uncoated and coated carbon fiber composites in the longitudinal direction of the fiber were measured using a three-point bending test according to ASTM D790-03 and ASTM D2344, respectively. The specimen dimensions were 50.8 mm in length and 12.5 mm in width for flexural tests and 15 mm in length and 7.5 mm in width for ILSS tests. An Instron 2204 machine was used to perform both tests, with a 1 kN load cell for flexural tests and 50 kN for ILSS tests, at a speed of 1 mm/min. A minimum of five laminates were tested for each composite.

The interlaminar fracture toughness properties of the composites under Mode I static loading were determined using a double cantilever beam (DCB) test in accordance with the ASTM D5528 specifications. The specimen dimensions were 100 mm in length and 20 mm in width, with a 40 mm long pre-crack along the mid-plane. Two metallic hinges were bonded to the end of the specimen using a two-component epoxy adhesive (Araldite 2014–2) to withstand the peeling force of the load cell. The lateral surface of the specimen was coated with a spray developer (SKD-S2) and marked every 5 mm to observe crack growth. The test was performed by applying a tensile load to the pre-cracked end of the sample at a constant displacement crosshead rate of 1 mm/min using an MTS 858 mini Bionix. A camera (Canon EOS 70D) was used to monitor crack growth, taking pictures every 5 s. Mode I interlaminar fracture toughness (G_I) was calculated using the modified beam theory (MBT) method:

$$G_I = \frac{3P\delta}{2b\,(a + |\Delta|)} \tag{1}$$

where P is the force (N), δ is the displacement (mm), a is the crack length (mm), b is the specimen width (mm), and Δ is the effective extent of delamination, which corrects the rotation of the arms of the DCB.

After the DCB test, the delaminated composites were healed in a hydraulic press at 150 °C for 120 min and a pressure (5 bar) was applied to ensure contact between the cracked surfaces. The healing efficiency was improved by applying pressure to the delaminated composite, because it minimized the crack volume that had to be repaired [20]. The healed samples were then cooled to room temperature and retested under the same conditions described above. Self-healing efficiency was calculated as the ratio between the fracture toughness in the repaired and virgin states:

$$n\ (\%) = \frac{G_I^{repaired}}{G_I^{virgin}} \cdot 100 \tag{2}$$

In addition, SEM was used to evaluate the healing of the damaged surface interphase. For this purpose, a TM3000 Tabletop Microscope was used without sputter coating with gold.

3. Results and discussion

3.1. Coating of carbon fibers with EMAA

Fig. 2 a shows the size distribution of the EMAA nanoparticles obtained by DLS between 50 and 300 nm, with a maximum value of approximately 120 nm. Such a small particle size can be attributed to the high precipitation rate caused by cold quenching of the solution compared to previously reported results under ambient conditions [38]. The polymer particle size depends on the cooling rate rather than on the polymer concentration [39]. Therefore, the EMAA solution was cooled in an ice bath to accelerate nucleation and, thus, reduce the EMAA particle size. The smaller the particle size, the easier the spraying process and the better the adhesion to the carbon fiber surface. However, when the particles are dried after the spraying, large size aggregates are formed (Fig. 2 b-d).

The cooling step plays a decisive role in the morphology of the EMAA-coated fibers. When the EMAA was sprayed from a hot solution, that is, when the EMAA was still dissolved, the coating had a similar appearance to that achieved with the cooled solution, acquiring a white hue (Fig. 3) However, irregular flakes were observed on the fibers, resulting in a heterogeneous coating (Fig. 4 middle). By spraying the cold solution, EMAA nanoparticles uniformly and homogeneously coated the entire fiber surface owing to their large surface area. The nanoparticles formed well-defined submicron-sized raspberry-like particles [38] (Fig. 4 bottom). Additionally, they were perfectly bonded to the fiber surface as they could be manipulated without damaging the coating. Thus, spray coating increased the roughness of the fiber and provided a scalable procedure for introducing EMAA nanoparticles into the composite.

3.2. Mechanical and healing properties of composites

Table 2 summarizes the mechanical behavior of the uncoated and EMAA-coated carbon fiber composites in flexural, ILSS, and DCB tests. The EMAA-coated fibers exhibited flexural and ILSS properties similar to those of the uncoated laminate, with a slight decrease within experimental error. Previous studies have reported a significant deterioration in the material properties when incorporating EMAA [14,26,29,32,40]. Gao *et al.* [26] reported a decrease of 43 % in flexural strength and 29 % in ILSS when EMAA was incorporated as a mesh over the fiber. While, Azevedo *et al.* [29] reported an average strength reduction of 22 % for samples containing 5–15 wt% EMAA as healing agent in the mid-plane of carbon fiber-epoxy composites. Therefore, the obtained properties are ascribed to the well-adhered EMAA particles on the fibers, resulting in a strong interface.

The DCB test evidences the positive effect of the presence of EMAA, yielding higher fracture energies with a toughness increase of 260 %. Similar improvements have been reported in previous studies. Loh *et al.* [30] observed that when EMAA was incorporated as filaments, the G_I increased from 1000 J/m^2 to 3530 J/m^2. Wang *et al.* [14] reported increments of 106 % when the EMAA was added in the form of patches into the interlayer region of epoxy/carbon fiber laminates. This phenomenon is seemingly due to the high ductility of the EMAA. When subjected to tensile deformation, Mode I traction loads oppose the crack opening, lowering the stress applied at the crack tip and, thereby, increasing Mode I fracture toughness [13,21].

The DCB test was also used to study the healing capacity of the EMAA-coated carbon fibers (Fig. 5). An example of the load vs displacement curves for the coated carbon fiber composites for three healing cycles is shown in Fig. 5 a. The composites exhibited the same behavior for the three cycles; the force increased linearly in the early stages and gradually decreased as the crack propagated. Furthermore, the maximum force decreased in the first healing cycle and stabilized in subsequent cycles, as reported by Shanmugam et al. [24]. As expected, the uncoated fiber composites subjected to the same healing conditions

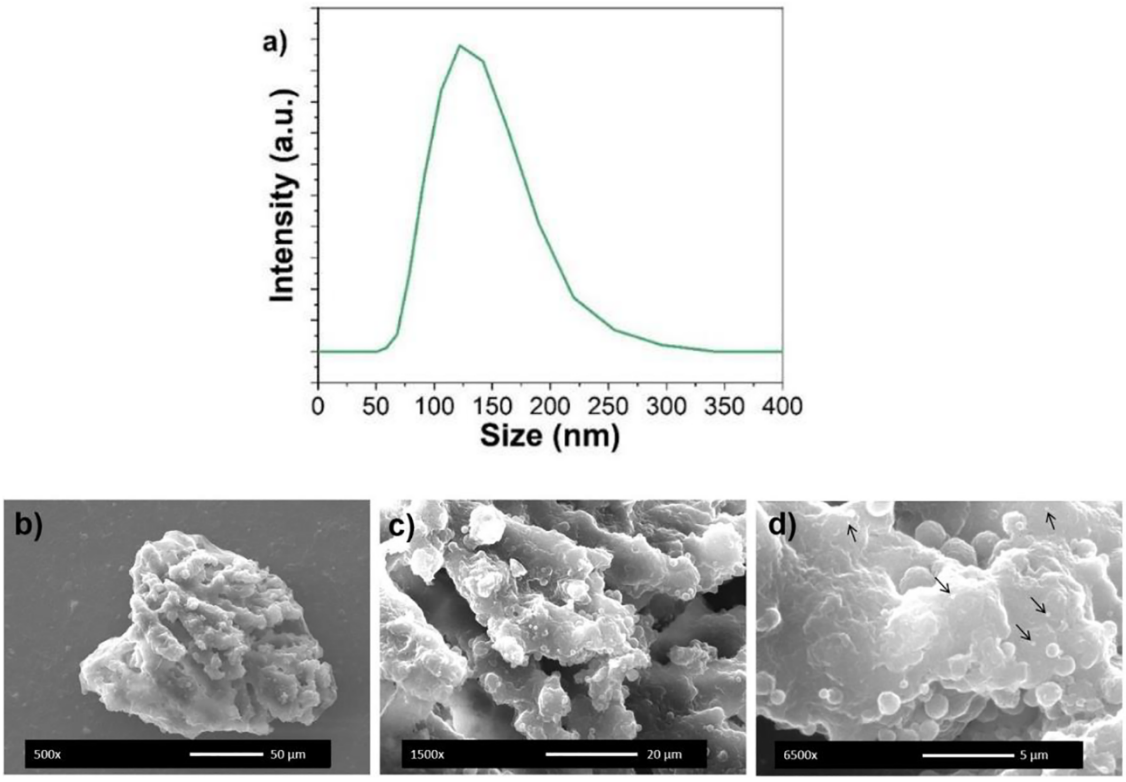

Fig. 2. a) Particle size distribution of EMAA obtained by DLS; (b-d) SEM images of EMAA particles at different magnifications. Arrows indicate particles smaller than 200 nm.

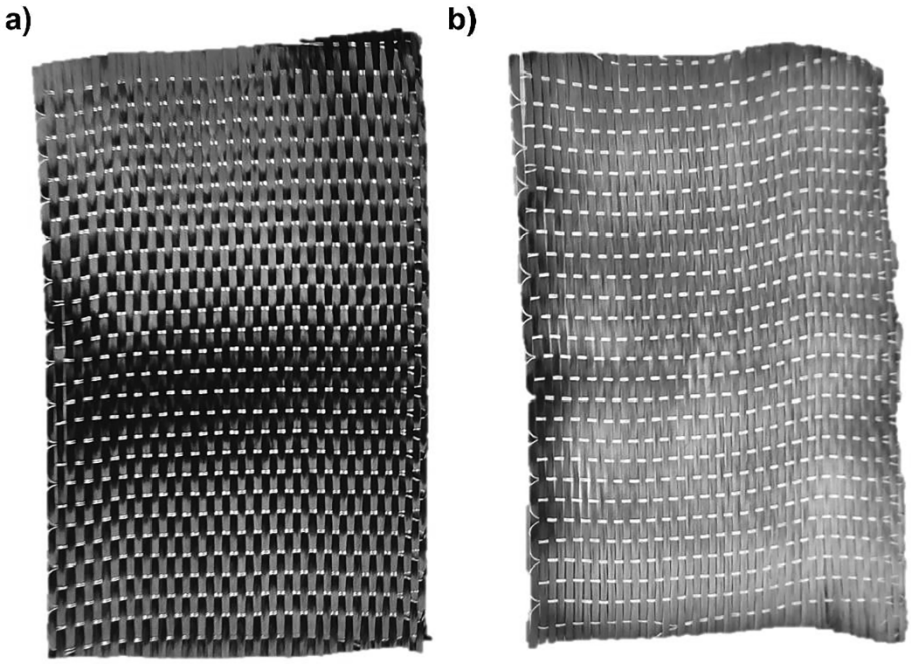

Fig. 3. Images of a) uncoated carbon fiber and b) EMAA-coated carbon fiber.

did not exhibit any healing behavior.

The Mode I strain energy release rate, G_I, was calculated at different crack lengths once they reached a constant value. The G_I value gradually decreased with increasing number of healing cycles (Fig. 6). However, the G_I value after the first healing cycle was higher than that of the uncoated fiber composite. The healing efficiency was calculated using Eq. (2), using the force and G_I values obtained for each cycle. The healing efficiency decreases as the number of repair cycles increases from 46 % in the first cycle to 28 % and 15 % in the second and third cycles, respectively. Notably, even after the third healing cycle, the composite exhibited acceptable G_I values. Shanmugam *et al.* [24] reported a similar behavior when EMAA was incorporated as a polymer

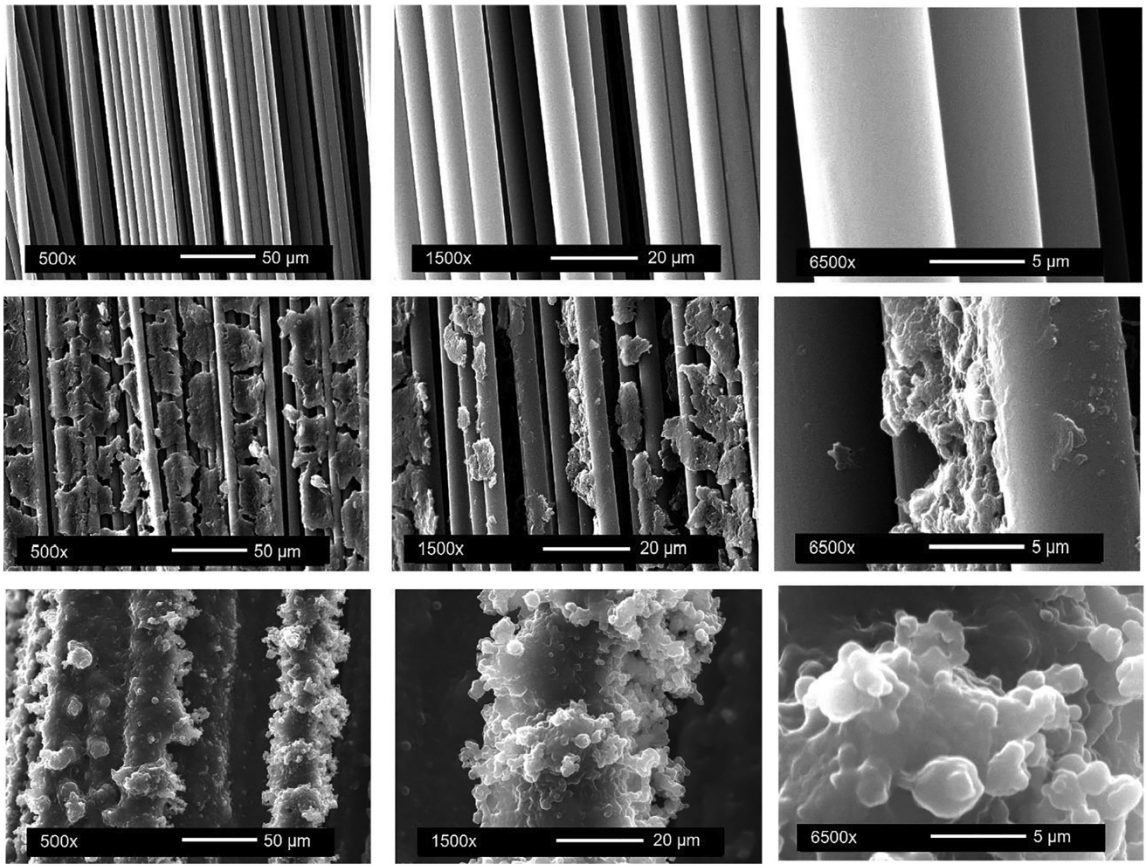

Fig. 4. SEM images of (top) uncoated carbon fibers, (middle) coated carbon fiber sprayed with hot dissolution of EMAA, and (bottom) coated carbon fiber sprayed with cold dissolution of EMAA.

Table 2
Mechanical properties of uncoated and EMAA-coated carbon fiber laminates.

	Flexural strength (MPa)	Young's modulus (GPa)	ILSS (MPa)	G_I (J/m^2)
Uncoated CF	897 ± 83	63 ± 6	47 ± 4	1073 ± 84
EMAA-coated CF	787 ± 87	59 ± 6	43 ± 2	2758 ± 197

interlayer in a carbon fiber reinforced epoxy composite. They observed recoveries of 75.8 %, 36.9 %, and 27.6 % for three healing cycles, respectively. They attributed this decrease to the depletion of the reactive components, that is, the hydroxyl groups in the resin and the acid groups in the EMAA, during the healing cycles. However, a plausible explanation to this behavior can be the formation of "bridges" that act by connecting the two surfaces of the crack (Fig. 7). When temperature is applied during the healing cycle, the EMAA flows to the crack owing to a pressure delivery mechanism. After cooling, the thermoplastic remains tightly adhered to the matrix, forming bridging stitches [1,20,41].

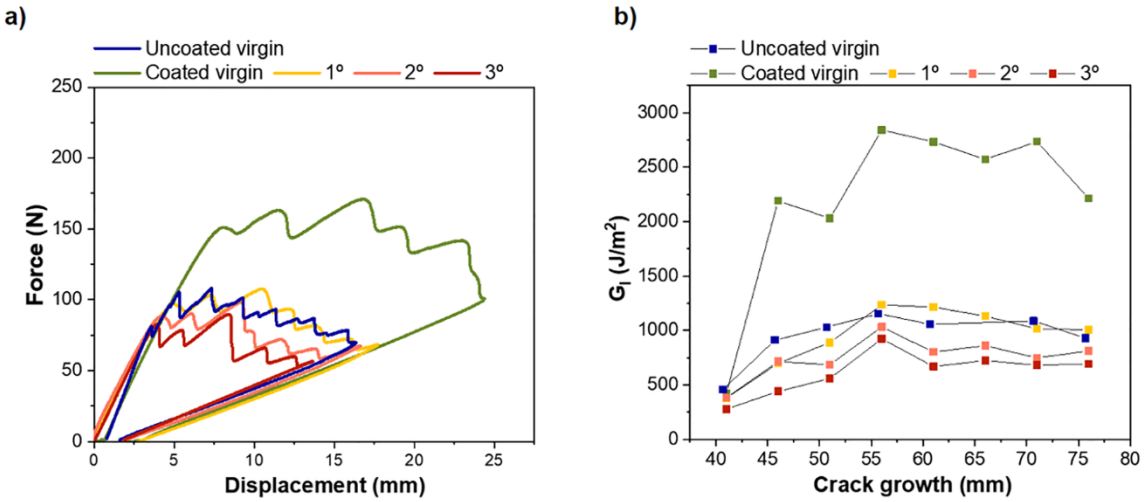

Fig. 5. Healing cycles of EMAA-coated samples from the DCB test: a) load–displacement curves and b) Mode I crack growth resistance curves.

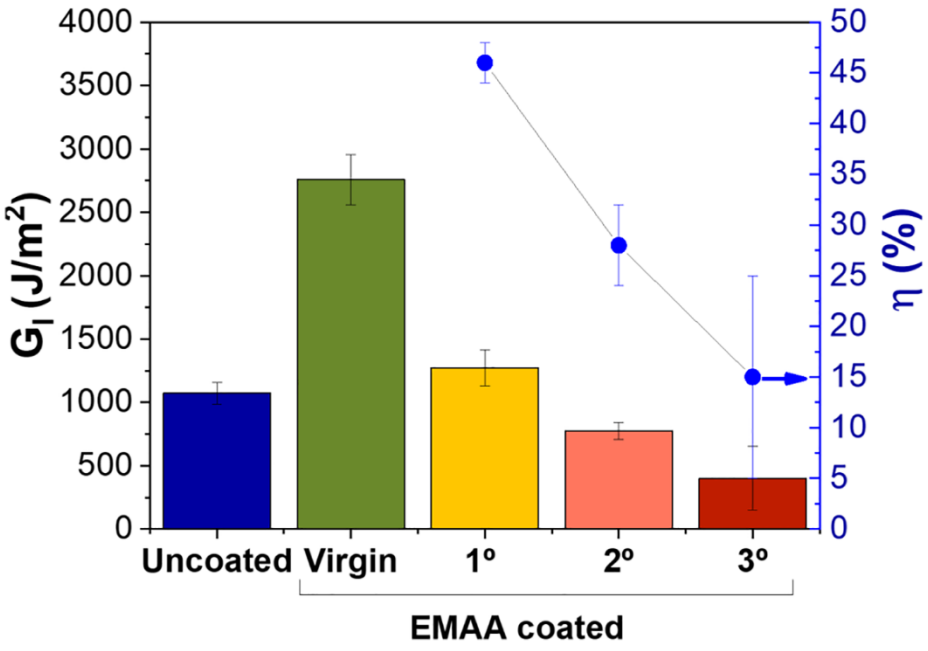

Fig. 6. Values of G_I (left) and healing efficiency (right) for uncoated and EMAA-coated carbon fiber composites after three healing cycles.

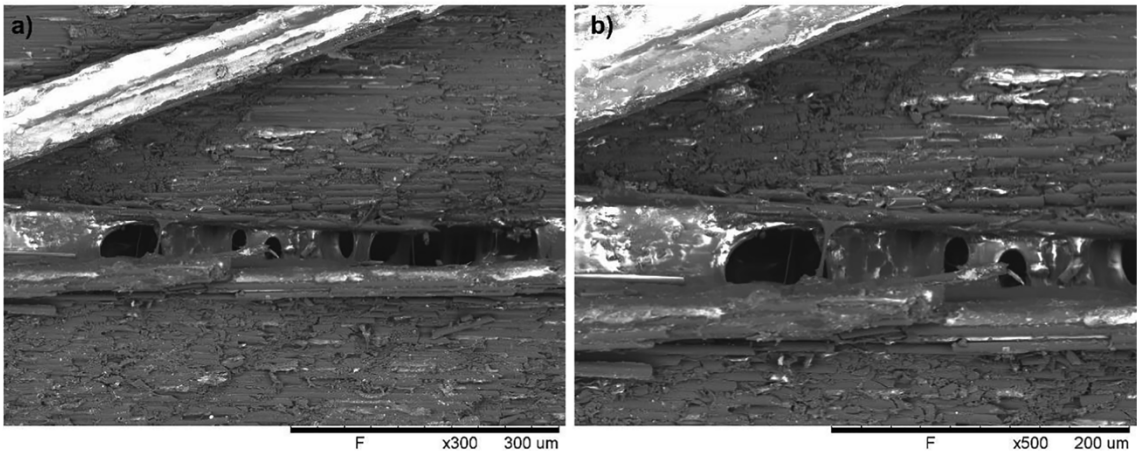

Fig. 7. SEM images of a repaired EMAA-coated carbon fiber composite at different magnifications.

This bridging reduces the stress acting on the crack during testing and leads to an increase in fracture toughness. In addition to the formation of these bridges, reactions occur between the epoxy resin and EMAA, contributing to the strong interfacial adhesion, as previously described in the literature [42].

Fig. 8 shows the schematic of the healing process. When the damaged material is subjected to pressure and temperature, the thermoplastic material flows through the crack, and ligaments are formed between the two damaged surfaces. Both these mechanisms promote healing. During the rupture of the material, the ligaments break and the crack propagates to its initial state. This cycle is reversible, as observed in this work, enabling several cycles of rupture and repair, but with a reduction in the percentage of healing efficiency due to the depletion of the reactive groups with the healing cycles.

4. Conclusions

In this study, we presented an innovative methodology for the incorporation of EMAA-coated fibers in epoxy composites. The spray-coating procedure had some advantages compared to those previously reported for conferring both healing capacity and good mechanical properties to an epoxy-based composite. First, the EMAA coating can easily be implemented on an industrial scale and be considered as a functional sizing, where the EMAA particles are evenly distributed over the surface of the fibers and exhibit good adhesion, which ensures a robust coating when handling the fibers. Second, the coating did not drastically affect the mechanical properties, with a noteworthy increase of 260 % in interlaminar fracture toughness. The EMAA-coated fibers also promoted the healing capacity of the composites owing to the inherent flow capacity of the thermoplastic and the formation of interfacial bridging between the two damaged interphases, with recoveries of 46, 28, and 15 % after three healing cycles, respectively.

CRediT authorship contribution statement

Mónica Peñas-Caballero: Conceptualization, Data curation, Formal analysis, Investigation, Methodology, Visualization, Validation, Writing – original draft, Writing – review & editing. **Enrico Chemello:** Data curation, Formal analysis, Investigation, Validation, Writing – original draft. **Antonio Mattia Grande:** Methodology, Supervision, Validation,

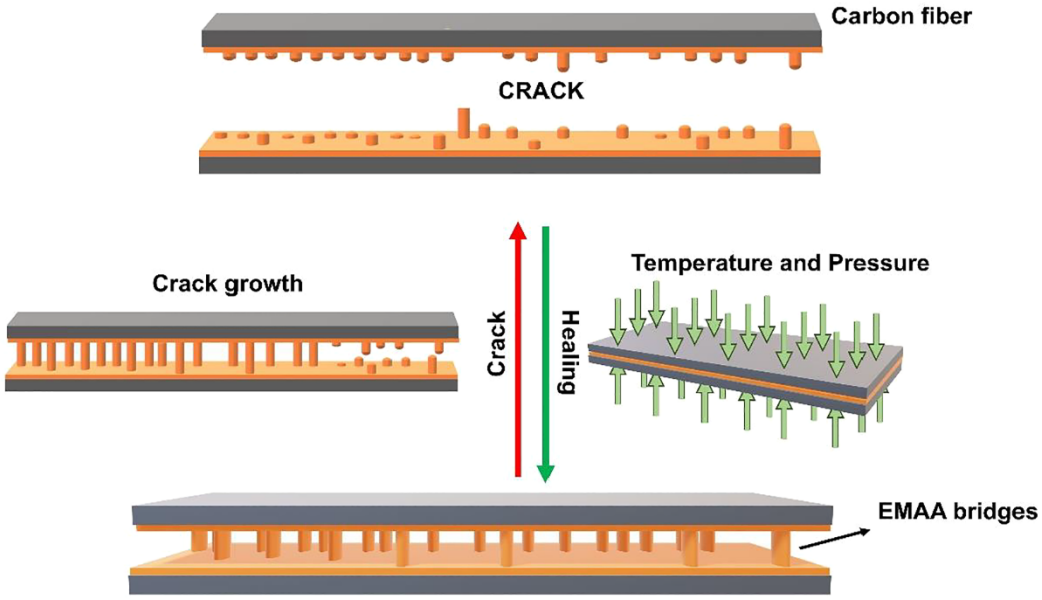

Fig. 8. Scheme of the healing process.

Writing – review & editing. **Marianella Hernández Santana:** Conceptualization, Methodology, Supervision, Validation, Visualization, Writing – review & editing. **Raquel Verdejo:** Conceptualization, Methodology, Supervision, Validation, Visualization, Writing – review & editing, Funding acquisition, Project administration. **Miguel A. Lopez-Manchado:** Conceptualization, Methodology, Supervision, Validation, Visualization, Writing – review & editing, Funding acquisition, Project administration.

Declaration of Competing Interest

The authors declare that they have no known competing financial interests or personal relationships that could have appeared to influence the work reported in this paper.

Data availability

Data will be made available on request.

Acknowledgments

This research was funded by the Spanish Research Agency, grant numbers PID2019-107501RB-I00/AEI/10.13039/501100011033 and RYC-2017-22837. Mónica Peñas-Caballero thanks a Predoctoral contract (BES-2017-079899).

References

[1] Pingkarawat K, Bhat T, Craze DA, Wang CH, Varley RJ, Mouritz AP. Healing of carbon fibre-epoxy composites using thermoplastic additives. Polym Chem 2013;4(18):5007–15.
[2] Pingkarawat K, Wang CH, Varley RJ, Mouritz AP. Mechanical properties of mendable composites containing self-healing thermoplastic agents. Compos Part A Appl Sci Manuf 2014;65:10–8.
[3] Jony B, Roy S, Mulani SB. Fracture resistance of in-situ healed CFRP composite using thermoplastic healants. Mater Today Commun 2020;24:101067.
[4] Van der Zwaag S, Grande AM, Post W, Garcia SJ, Bor TC. Review of current strategies to induce self-healing behaviour in fibre reinforced polymer based composites. Mater Sci Technol 2014;30(13):1633–41.
[5] Islam S, Bhat G. Progress and challenges in self-healing composite materials. Mater Adv 2021;2(6):1896–926.
[6] Jony B, Thapa M, Mulani SB, Roy S. Experimental characterization of shape memory polymer enhanced thermoplastic self-healing carbon/epoxy composites. AIAA Scitech (2019) Forum 2019:1–11.
[7] Sánchez-Romate XF, Sans A, Jiménez-Suárez A, Prolongo SG. The addition of graphene nanoplatelets into epoxy/polycaprolactone composites for autonomous self-healing activation by Joule's heating effect. Compos Sci Technol 2021;213:108950.
[8] Hayes SA, Zhang W, Branthwaite M, Jones FR. Self-healing of damage in fibre-reinforced polymer-matrix composites. J R Soc Interface 2007;4(13):381–7.
[9] Zako M, Takano N. Intelligent Material Systems Using Epoxy Particles to Repair Microcracks and Delamination Damage in GFRP. J Intell Mater Syst Struct 1999;10(10):836–41.
[10] Meure S, Wu DY, Furman S. Polyethylene-co-methacrylic acid healing agents for mendable epoxy resins. Acta Mater 2009;57(14):4312–20.
[11] Peterson AM, Kotthapalli H, Rahmathullah MAM, Palmese GR. Investigation of interpenetrating polymer networks for self-healing applications. Compos Sci Technol 2012;72(2):330–6.
[12] Meure S, Furman S, Khor S. Poly[ethylene-co-(methacrylic acid)] healing agents for mendable carbon fiber laminates. Macromol Mater Eng 2010;295(5):420–60.
[13] Varley RJ, Parn GP. Thermally activated healing in a mendable resin using a non woven EMAA fabric. Compos Sci Technol 2012;72(3):453–60.
[14] Wang CH, Sidhu K, Yang T, Zhang J, Shanks R. Interlayer self-healing and toughening of carbon fibre/epoxy composites using copolymer films. Compos Part A Appl Sci Manuf 2012;43(3):512–8.
[15] Yang T, Wang CH, Zhang J, He S, Mouritz AP. Toughening and self-healing of epoxy matrix laminates using mendable polymer stitching. Compos Sci Technol 2012;72(12):1396–401.
[16] Pingkarawat K, Wang CH, Varley RJ, Mouritz AP. Self-healing of delamination cracks in mendable epoxy matrix laminates using poly[ethylene-co-(methacrylic acid)] thermoplastic. Compos Part A Appl Sci Manuf 2012;43(8):1301–7.
[17] Hargou K, Pingkarawat K, Mouritz AP, Wang CH. Ultrasonic activation of mendable polymer for self-healing carbon-epoxy laminates. Compos B Eng 2013;45(1):1031–9.
[18] Yang T, Du Y, Li ZM, Wang CH. Mechanical properties of self-healing carbon fiber-epoxy composite stitched with mendable polymer fiber. Polym Polym Compos 2014;22(3):329–36.
[19] Almuhammadi K, Alfano M, Yang Y, Lubineau G. Analysis of interlaminar fracture toughness and damage mechanisms in composite laminates reinforced with sprayed multi-walled carbon nanotubes. Mater Des 2014;53:921–7.
[20] Pingkarawat K, Wang CH, Varley RJ, Mouritz AP. Healing of fatigue delamination cracks in carbon-epoxy composite using mendable polymer stitching. J Intell Mater Syst Struct 2014;25(1):75–86.
[21] Pingkarawat K, Mouritz AP. Stitched mendable composites: Balancing healing performance against mechanical performance. Compos Struct 2015;123:54–64.
[22] Ladani RB, Pingkarawat K, Nguyen ATTT, Wang CH, Mouritz AP. Delamination toughening and healing performance of woven composites with hybrid z-fibre reinforcement. Compos Part A Appl Sci Manuf 2018;110:258–67.
[23] Kostopoulos V, Kotrotsos A, Baltopoulos A, Tsantzalis S, Tsokanas P, Loutas T, et al. Mode II fracture toughening and healing of composites using supramolecular polymer interlayers. Express Polym Lett 2016;10(11):914–26.
[24] Shanmugam L, Naebe M, Kim J, Varley RJ, Yang J. Recovery of Mode I self-healing interlaminar fracture toughness of fiber metal laminate by modified double cantilever beam test. Compos Commun 2019;16:25–9.
[25] Zhang XF, Li D, Liu K, Tong J, Yi XS. Flexible graphene-coated carbon fiber veil/polydimethylsiloxane mats as electrothermal materials with rapid responsiveness. Int J Lightweight Mater 2019;2(3):241–9.

[26] Gao Ya, Liu L, Wu Z, Zhong Z. Toughening and self-healing fiber-reinforced polymer composites using carbon nanotube modified poly (ethylene-co-methacrylic acid) sandwich membrane. Compos Part A Appl Sci Manuf 2019;124:105510.
[27] Ladani RB, Nguyen ATTT, Wang CH, Mouritz AP. Mode II interlaminar delamination resistance and healing performance of 3D composites with hybrid z-fibre reinforcement. Compos Part A Appl Sci Manuf 2019;120:21–32.
[28] Ladani RB, Wang CH, Mouritz AP. Delamination fatigue resistant three-dimensional textile self-healing composites. Compos Part A Appl Sci Manuf 2019;127:105626.
[29] Azevedo A, Fernandez F, Fábio S, Ferreira EPC, Daniel J, Melo D, et al. Addition of poly (ethylene-co-methacrylic acid) (EMAA) as self-healing agent to carbon-epoxy composites. Compos Part A Appl Sci Manuf 2020 2020;137:106016.
[30] Loh TW, Ladani RB, Orifici A, Kandare E. Ultra-tough and in-situ repairable carbon/epoxy composite with EMAA. Compos Part A Appl Sci Manuf 2021;143:106206.
[31] Haramina T, Pugar D, Ivančević D, Smojver I. Mechanical properties of poly (Ethylene-co-methacrylic acid) reinforced with carbon fibers. Polymers 2021;13(1):165.
[32] OuYang Q, Wang X, Liu L. High crack self-healing efficiency and enhanced free-edge delamination resistance of carbon fibrous composites with hierarchical interleaves. Compos Sci Technol 2022;217:109115.
[33] Snyder AD, Phillips ZJ, Turicek JS, Diesendruck CE, Nakshatrala KB, Patrick JF. Prolonged in situ self-healing in structural composites via thermo-reversible entanglement. Nat Commun 2022;13:6511.
[34] Guerra ÉSS, Silva BL, Melo JDD, Kalinka G, Barbosa APC. Microscale evaluation of epoxy matrix composites containing thermoplastic healing agent. Compos Sci Technol 2023;232:109843.
[35] Meure S, Wu DY, Furman SA. FTIR study of bonding between a thermoplastic healing agent and a mendable epoxy resin. Vib Spectrosc 2010;52(1):10–5.
[36] Chen B, Cai H, Mao C, Gan Y, Wei Y. Toughening and rapid self-healing for carbon fiber/epoxy composites based on electrospinning thermoplastic polyamide nanofiber. Polym Compos 2022;43(5):3124–335.
[37] Kostopoulos V, Kotrotsos A, Sousanis A, Sotiriadis G. Fatigue behaviour of open-hole carbon fibre/epoxy composites containing bis-maleimide based polymer blend interleaves as self-healing agent. Compos Sci Technol 2019;171:86–93.
[38] Huang HC, Zacharia NS. Layer-by-layer rose petal mimic surface with oleophilicity and underwater oleophobicity. Langmuir 2015;31(2):714–20.
[39] Kim KJ. Nano/micro spherical poly(Methyl methacrylate) particle formation by cooling from polymer solution. Powder Technol 2005;154(2–3):156–63.
[40] Li G, Li P, Zhang C, Yu Y, Liu H, Zhang S, et al. Inhomogeneous toughening of carbon fiber/epoxy composite using electrospun polysulfone nanofibrous membranes by in situ phase separation. Compos Sci Technol 2008;68(3-4):987–94.
[41] Pingkarawat K, Wang CH, Varley RJ, Mouritz AP. Healing of fatigue delamination cracks in carbon – epoxy composite using mendable polymer stitching. J Intell Mater Syst Struct 2014;25(1):75–86.
[42] Meure S, Varley RJ, Wu DY, Mayo S, Nairn K, Furman S. Confirmation of the healing mechanism in a mendable EMAA-epoxy resin. Eur Polym J 2012;48(3):524–31.